Earth and Planetary Science
https://journals.nasspublishing.com/index.php/eps

RESEARCH ARTICLE

A Small Impact Crater in the Dhofar Mountains, Sultanate of Oman: Surface Expression from Satellite Imagery and Cues from the Profiles of ICESat-2 Photons

Giribabu Dandabathula [1*] **, *Omkar Shashikant Ghatage*** [1] **, *Subham Roy*** [1] **, *Apurba Kumar Bera*** [1] **, *Sushil Kumar Srivastav*** [2]

[1] *Regional Remote Sensing Centre - West, National Remote Sensing Centre, Indian Space Research Organisation, Jodhpur 342005, India*

[2] *Regional Centres, National Remote Sensing Centre, Indian Space Research Organisation, New Delhi 110049, India*

ABSTRACT

This study discovered a surface expression of one small impact crater on the slopes of the Dhofar Mountains, Sultanate of Oman. This research utilized high-resolution satellite imagery, a digital elevation model, and ICESat-2 photon data to determine the geomorphological features of the impact crater. Elevation profiles from the ICESat-2 photons highlighted the crater's rim structure with high precision. Also, the structure of this impact crater was crosschecked with a confirmed crater on similar geological settings on Mars using HiRise imagery and numerical simulations. Additionally, a scaled sandbox experiment ensured the simulation of the impact mechanism on slopes. The identified impact crater is a simple type (non-complex) with a nearly bowl-shaped depression having a raised rim structure and a maximum diameter of ∼259 m. However, bearing its location on a sloped terrain and at the edge of the gorge's cliff-top, this elliptical crater remained crescent, with the deepest point shifted downhill. Notably, features related to the crater's structure, such as the rim, the floor's deepest point, and a tongue-like landslide at the downhill, are consistent with the numerical simulations and corroborate the results from the lab-based ex-

*CORRESPONDING AUTHOR:
Giribabu Dandabathula, Regional Remote Sensing Centre - West, National Remote Sensing Centre, Indian Space Research Organisation, Jodhpur 342005, India; Email: dgb.isro@gmail.com

ARTICLE INFO
Received: 7 November 2024 | Revised: 11 March 2025 | Accepted: 17 March 2025 | Published Online: 31 March 2025
DOI: https://doi.org/10.36956/eps.v4i1.1454

CITATION
Dandabathula, G., Ghatage, O.S., Roy, S., et al., 2025. A Small Impact Crater in the Dhofar Mountains, Sultanate of Oman: Surface Expression from Satellite Imagery and Cues from the Profiles of ICESat-2 Photons. Earth and Planetary Science. 4(1): 10–25. DOI: https://doi.org/10.36956/eps.v4i1.1454

COPYRIGHT
Copyright © 2025 by the author(s). Published by Nan Yang Academy of Sciences Pte. Ltd. This is an open access article under the Creative Commons Attribution-NonCommercial 4.0 International (CC BY-NC 4.0) License (https://creativecommons.org/licenses/by-nc/4.0/).

periments. The crater's ellipticity and depth-to-diameter ratio agree with the mechanisms involved in impact crater formation on slopes. This impact crater is one of the rarest on Earth, uniquely located on sloped terrain, and is the first to be reported through this article.

Keywords: Small Impact Crater; Dhofar Mountains; Sultanate of Oman; Elliptical Crater; Crescent Crater; Impact Craters on Slopes; Salalah

1. Introduction

Intrinsic geological processes like plate tectonic induced earthquakes, volcanoes, slope failure/landslides, subsidence/sinking of land, tsunamis and rapid-hydrological surface runoff, and aeolian-weathering episodes will be responsible for sculpting the surface geomorphology of planetary objects [1]. During these geological phenomena, significant energy gets released, resulting in a scar or a mark of surface morphological change; the greater the magnitude of the disturbing force, the more complex the morphological change in the landscape [2].

On the other hand, impact cratering is an extrinsic geological process that happens on the planetary surfaces due to the crash landing of high-velocity extraterrestrial objects from space like a meteorite, a separated object of orbiting asteroid or traveling comet, and space debris; the phenomenon results in an energy transfer mechanism where the kinetic energy of the impactor is transferred into heat, fracturing, and displacement of material or material energy of the target surface [3–6]. While the impactor is a significantly smaller object than the planet, the course outcome can be a pit or a crater [7, 8]. Impact pits are formed when extraterrestrial objects of relatively smaller size (like micrometeoroids of a centimeter to a sub-meter sized) with insufficient velocity crash lands on planetary surfaces and remain intact. Impact craters are formed by incoming meteorites with cosmic velocity colliding on a planetary surface, inducing shock metamorphism in the target material [8–10].

The cratering process and the final shape of the crater depend on various parameters of the colliding extraterrestrial object (like size, velocity, projectile, shape, and composition – rock to ingots or metal alloys) and also on the geological structure and strength of the target surface [8, 11]. The target's gravitational field controls the impactor's acceleration, influencing the collision's magnitude and, further, the crater's shape [12–14]. Unlike conventional endogenic processes, the impact-cratering process will be completed within a few seconds if the impact is due to smaller extraterrestrial objects, while for larger bodies, it is not more than 100 seconds [14–16].

The process of crater formation includes three sequential events: (1) contact and compression phase, (2) excavation, and (3) modification phase [8, 13, 14]. The contact and compression stage gets initiated once there is contact of an impacting body with the planetary surface and is the briefest of all the three stages. This stage redistributes the kinetic energy of the impacting projectile into internal energies of the impactor and the target surface, generating shock waves that develop from the point of contact. The stage ends after the shock compression of the impactor has been wholly unloaded through vaporization, melting, and ejected from the cavity.

During the first moments in the excavation stage, the shock wave forms in the target and expands away from the impact site, compressing and accelerating the material it encounters. The material in the target moves along outward directions that are approximately radial to the point of impact. During the subsequent excavation stage, the kinetic energy imparted to the target rocks by the interaction of the shock and rarefaction waves leads to particle velocities in the target rocks, with trajectories that define a flow field, combined with downward and outward physical compression of the target rocks, resulting in the formation of a transient cavity. The modification stage begins when the excavation stage ends and the transient crater has grown to its maximum size. During this stage, the inward and upward material motion results in a complex intermixture of breccia and impact melt inside the crater depression. The modification stage is driven by gravity, rock mechanics, and the rebound of the transient crater floor. Enough literature is

available on the mechanics of impact cratering from the works of Osinski et al., Kenkmann et al., and Melosh & Ivanov [8, 13, 14].

Though, to a good approximation, the impact occurs as a point source, the cratering mechanism yields two types of craters – simple and complex [13, 16]. Simple and complex impact craters have fundamental differences in morphology and structure, both being a function of size. Simple craters generally have a bowl-shaped morphology with a raised crater rim, while complex craters have terraced rims and an uplifted central portion of the crater floor. With increasing size, complex craters are further subdivided into central peaks, peak-ring craters, and multi-ring basins based on the morphology of the uplifted target rocks [8, 13]. Works from Osinski et al. and Kenkmann et al. provide satellite imagery-based illustrations of various impact craters that can be formed on planetary bodies [8, 13]. Crater depth (d) is the vertical distance from the deepest point on the floor to the plane passing through the rim height, and the diameter (D) is the outermost raised rim-to-rim diameter. Generally, the depth-diameter (d/D) ratio of large samples of simple craters ranges from 1:3 to 1:7, while for the complex craters, the d/D ratio ranges from ~1:10 to 1:20 [8]. The rim is composed mainly of broken rock debris and forms close to the angle of repose of loose rock debris - a mechanically plausible process [14]. In general, the shape of the crater rim is largely insensitive to the impact trajectory and remains circular due to the symmetric distribution of the ejecta blanket [13, 17, 18]. But for oblique impacts (say for angle <45°), the ejecta blanket becomes asymmetric, while for <25°, a forbidden zone develops in the upper range portion of the eject blanket, and the crater rim is depressed in that direction. The presence of a forbidden zone can indicate the direction of the impactor, which, as a whole, is a region in an impact crater where no ejecta gets deposited. The crater rim becomes saddle-shaped when the projectile is <15°, and while <10° degrees, the rim becomes elongated in the direction of impact, and the ejecta forms a "butterfly" pattern [13, 17, 18]. Most recorded impact craters on the planetary surfaces are circular, and only countable elliptical craters are reported on Mars, Moon, and Venus [8, 13, 17, 18].

Significant understanding of the impact cratering mechanism has occurred due to the advancements in space technology and the availability of satellite imagery acquired over planetary bodies like the Moon and Mars [19, 20]. However, on Earth, the state of impact craters might have eroded to some degree such that the original form of the crater is modified or even no longer present to recognize [8]; the reason can be attributed to intrinsic geological processes, weathering, and anthropogenic activities, among others. Thus, it is not easy to recognize the craters in an unpreserved state through field studies or remote sensing. However, records of the impact craters on Earth are critical to understanding impact events' processes and effects. A systematic collection of all the confirmed impact craters on Earth is available online for scientific fraternity at https://www.impactearth.com [8]. Remote sensing methods enable us to interpret and recognize the surface expression of a crater in satellite imagery; however, the crater's genesis and impact event analogy can be confirmed only through extensive fieldwork and analyzing the samples available at the crater's location [21, 22].

The presence of impact craters in a region provides an opportunity to enhance the scientific advancement and understanding of extraterrestrial mechanisms, as they often have very peculiar ecosystems surrounding them. Moreover, alien minerals near the impact craters can boost the region's economic prosperity along with the benefits of accruing the potential of tourism [23–25].

The authors of this research discovered a surface expression of a small impact crater in the Dhofar Mountains, located in the Dhofar Governorate, Sultanate of Oman. The primary objective of the present study is to determine the geomorphological features of this newly discovered impact crater; for this, we utilized various high-resolution satellite imagery, including archived imagery acquired originally for reconnaissance survey, as part of our analysis. Additionally, Light Detection and Ranging (LiDAR) based high-resolution elevation profiles were used to understand the intricate details of this surface expression at a sub-meter level. The peculiarity of this impact crater is that it lies on sloped terrain and the edge of a gorge's cliff-top; thus, an experiment was performed to simulate the impact cratering on the slopes

in a scaled sandbox setup that enabled simulation of its final form. There are records of small impact craters on the Moon, Mars, and Venus, which are elliptical and have smaller rim-to-rim diameters, especially secondary craters (i.e., smaller craters within a large crater system). Simple and elliptical craters are highly rare on the Earth [8]. The uniqueness of this discovered elliptical impact crater is its location on an undulated (sloped) terrain, its rim structure is in a preserved state, and almost all of its attributes are in sync with the structural principles of simple (non-complex) impact craters that happen on that happens on sloped surfaces and herewith reported for the first time in this article.

2. Materials and Methods

2.1. Study Area

The Oman mountains are geologically famous for having the world's largest ophiolite complex, a thrust slice of oceanic crust and upper mantle formed 96–95 million years ago and emplaced onto the Arabian continental margin during the Late Cretaceous between 95 and 70 million years ago [26]. The Oman ophiolite played a significant role in geological studies, which resulted in the theory of plate tectonics proposed in the 1960s [26]. The Sultanate of Oman, a country on the southeastern coast of the Arabian Peninsula, overlooks the mouth of the Persian Gulf. Sultanate of Oman is surrounded by the great desert of the Rub al-Khali to the west, covering parts of Saudi Arabia, Yemen, and the United Arab Emirates. The south and east of Oman is entirely a coast adjoining the Arabian Sea. The southern province of Oman, Dhofar, is bounded by the Indian Ocean along the south, the Yemen border in the west, and the great sand sea of the Rub al-Khali or Empty Quarter to the north. The coastal region of Dhofar is dominated by the strike-slip faults along the Arabian plate margin [26]. The impact crater discovered in this research lies in the Dhofar Mountains located north of Salalah plains; the precise location of this small crater is 17°04'02.8"N, 53°55'06.8"E. Jardoom, located some 20 km to the northwest from Salalah is the nearest hamlet from this impact crater. **Figure 1** shows the map of the impact crater under investigation.

Dhofar Mountains experience mild temperatures and high precipitation due to the interplay of topographic relief and the Intertropical Convergence Zone (ICZ) position that delivers humid onshore winds to the coastal plain and its mountains during the summer months. Most steep escarpments rising 1000 m behind the coast trap the seasonal moist air, feeding the endemic woodland and grassland biomes with light precipitation [27]. Mainly, the hills are flourished with dragon trees and frankincense [26, 27]. Dhofar region is also influenced by tropical depressions that develop over the Indian Ocean; these depressions frequently breach the mountain escarpment and can unleash up to 540 mm of rain in a single event [27].

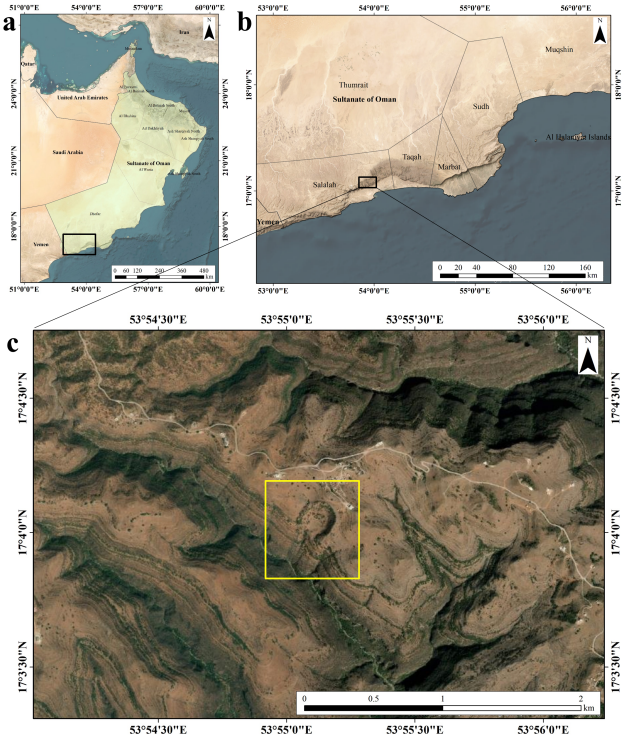


Figure 1. Location map of the impact crater identified on the Dhofar Mountains, ~20 km northwest of Salalah, Dhofar Governorate, Sultanate of Oman. (**a**) Administrative boundary of Sultanate of Oman; (**b**) Location of the Dhofar mountains chain and Salalah; (**c**) The small impact crater, as seen in satellite imagery acquired by LISS-IV onboard IRS ResourceSat-2A. The image acquisition date is 29 December 2023. The precise location of this small crater is 17°04'02.8"N, 53°55'06.8"E.

To the north of the Dhofar Mountains, the Nejd Plateau is a gently sloping tableland dissected by several prominent drainage systems that debouch into a large interior basin [27]. To the south of the Dhofar Mountains,

the Salalah coastal plains adjoin the Arabian Sea. The region where the small impact crater identified in this research is a massif (referred locally to as Jebel Qara) dominant with Tertiary and Cretaceous limestone and is primarily a gently undulating terrain, reaching a maximum height of ∼900 m above sea level [28–30]. The region's Geological description was reported earlier by Cremaschi et al. and Zerboni et al.; primarily, the massif is dissected by a dendritic system of valleys cut into the bedrock [29, 30].

2.2. Datasets

Remote sensing data enables the identification of the impact craters on the planetary surfaces based on their geomorphologic shapes. Numerous achievements have been made in identifying impact craters using remote-sensing images [8, 31]. However, the final confirmation to ascertain the status of an impact crater, specifically on Earth, needs expert fieldwork, collection and analysis of the samples, geophysical surveys, and a requirement for radiocarbon dating of materials found near the crater floor [8]. Interpretation keys to recognize the impact craters from satellite images are already well documented [32]; moreover, recent advancements in machine learning and deep learning have enabled the automatic detection of impact craters from satellite imagery [33–36].

In this research, multispectral data from the Indian Remote Sensing Satellite (IRS), namely Resourcesat-2A's Linear Imaging Self-Scanning Sensor-IV (LISS-IV), has been used to identify various features of this small impact crater. LISS-IV imagery is of 5.8 m spatial resolution containing reflectance from green (0.52–0.59 µm), red (0.62–0.68 µm), and near-infrared (0.77–0.86 µm) (https://www.isro.gov.in/RESOURCESAT_2A.html). ESRI's ArcGIS online base-maps (https://www.arcgis.com) and Google Earth (https://earth.google.com/web) support delivering imagery through OpenGIS Web Map Service (WMS) Interface Standards; thus, one can visualize various geospatial datasets, including satellite imagery using appropriate client software. In this research, basemaps (satellite imagery layer) from ESRI and Google Earth were used to understand the intricate details of surface expression given by the small impact crater reported in this research.

Declassified photoreconnaissance aerial/satellite images under the CORONA program by the U.S. from 1959 to 1972 are available for scientific applications [37]. Imagery from the KH-4B mission with 1.8 m spatial resolution, acquired on 01 May 1972 under the CORONA program, was used as material to verify the historical existence of the impact crater. The United States Geological Survey (USGS) Earth Explorer is a tool that allows users to search, discover, and order earth sciences data through an open-access mechanism. For this research, imagery acquired under the CORONA mission is downloaded from the USGS Earth Explorer tool, available at https://earthexplorer.usgs.gov/.

The High-Resolution Imaging Science Experiment (HiRise) camera, the most powerful digital imaging system flown beyond Earth's orbit, is carried onboard the Mars Reconnaissance Orbiter (MRO) spacecraft. It has produced a large number of color images of the surface of Mars with greater details due to its higher spatial resolution (up to ∼0.3 m) capability [38]. Researchers have identified new impact craters on Mars's surface, including those of <1 km diameter, using the HiRise imagery [39–41]. In this research, we have used HiRise imagery for the extent of the slopes of Tithonium Chasmato, a large Valles Marineris canyon system on Mars. An unnamed 3–4 km diameter Martian impact crater was highlighted earlier by Aschauer and Kenkmann, and the significance of this impact crater is that it mainly exists in a topography dominated by slopes [18]. The small impact crater described in this research is also located on slopes similar to that of the unnamed crater that is lying at the Tithonium Chasmato on Mars; thus, the known features of an identified impact crater from the HiRise imagery should enable us to relate the impact of topographic slopes on the crater's shape.

Digital Elevation Models (DEM), unlike satellite imagery, which contains surface reflectance/emittance values for a pixel, each grid cell has a height value representing physical surface elevation; thus, they enable understanding the variations in the terrain and help retrieve the characteristics of the topography for the extent of the study area. In complementary to satellite imagery, DEMs enable morphological studies of terrestrial

impact craters to an unprecedented level [42–44]. This research uses ALOS PALSAR global DEM, available at 12.5 m (https://asf.alaska.edu), to understand the detailed topographic information surrounding the identified small impact crater under investigation. Additionally, the World Hillshade layer available from ESRI (https://www.arcgis.com) is used to envisage the surface expression of the identified small-impact crater. In general, hillshade maps provide a realistic, 3D representation of terrain that's easy to understand and can be used to highlight subtle differences in topography.

Generally, the category of impact craters whose rim-to-rim distance is within a sub-kilometer is said to be small [8]. Extracting the intricate topographic details for small impact craters from the open-access DEMs with a grid size of 12.5 m and greater may fail to provide critical information about the crater's rim structure and variations in its floor. In such a situation, data from LiDAR-based elevations may be a better option. NASA's Ice, Cloud and land Elevation Satellite-2 (ICESat-2), a novel satellite with a solo sensor, ATLAS, was launched in September 2018 and has been operational since then [45]. The scientific fraternity has appreciated the unique capability of ICESat-2 in giving measurements for every 0.7 m along the track [46]. Combined with the ICESat-2's precision pointing and positioning information, the range measurements produce geolocation and elevations for all the successful laser photon returns from the Earth's surface [46]. A sequence of geolocated photons is of immense use to study the Earth's surface features through profiling [47]. In the first five years after the launch of ICESat-2, numerous research areas in the Earth sciences reported the significance and application capability of geolocated photon data - in fact, the geolocated photon data from ICESat-2 not only filled certain gap areas in the geospatial technologies but also unleashed novel applications for Earth sciences. Even though the science objectives of ICESat-2 are oriented towards observing the cryosphere, researchers have successfully used the geolocated photons in a variety of disciplines related to land, ice, sea ice, vegetation/canopy, inland surface water, and atmospheric studies in complementary with remote sensing imagery [48]. In this research, two acquisitions (referred to as Beam$_{ab}$ and Beam$_{pq}$) of ICESat-2 photon data that are available over the extent of the small impact crater (details mentioned in Table 1) were considered to generate 2D along-track elevation profiles over the crater's rim-to-rim. The usage of these profiles is briefed in the subsequent section.

The details of all the datasets used in this research and their relevance are mentioned in **Table 1**. Results from the numerical simulations and descriptions that have emphasized terrestrial impacts on the sloped surfaces by the earlier researchers were also considered to relate to the morphometric shape of the impact crater envisaged in this research [18, 49–52].

Additionally, simulating experiments of impact cratering on slopes provides information that helps to understand how such craters form; an experimental setup with a simulated landscape environment (in a sandbox - granular target surface) that of the crater as on Dhofar Mountains was made to verify the consequence of impact on slopes. The layers in the experimental landscape emulate having multiple strata representing the monocline folds of the Dhofar crater site (discussed in the subsequent sections). We use an oval-shaped glass paperweight of diameter 2.5 inches and weighing 300 grams as an impactor. The impactor is released from 15 feet height with a 45° angle (termed the most probable impact angle) and is accelerated by gravity. The target position was set to land only on the uphill slope near the edge of the cliff-top and avoid landing on the gorge's steep wall. The container dimensions are 1m x 1m, sufficiently accommodating all the impact effects within its dimensions. The scaled landscape design contains an uphill slope of $\sim$16° covered with granular material and the gorge's wall at a steep slope of $\sim$30°.

2.3. Methods

This research used high-resolution optical imagery from IRS Resourcesat-2A's LISS-IV and online satellite imagery base-maps to recognize the impact crater's primary geomorphologic characteristics. Optical satellite imagery from the Earth observation sensors can effectively identify the distinctive features of impact craters such as raised rim, basin floor, preservation state, and surrounding environs. Additionally, using image processing or GIS software, one can perform measurements

Table 1. Datasets used in detailing the small impact crater identified at the Dhofar mountain chain, ∼20 km northwest of Salalah, Dhofar Governorate, Sultanate of Oman.

Dataset	Specifications and Source	Relevancy
IRS Resourcesat-2A LISS-IV	Spatial resolution: 5.8 m Date of acquisition: 29 Dec. 2023 Source: https://bhoonidhi.nrsc.gov.in	To understand various spatial features of the small impact crater under investigation using false color and natural color composites
Online satellite imagery base-maps	Spatial resolution: < 0.5 m Web Mapping Services (WMS) available under ArcGIS software (https://www.arcgis.com) and Google Earth (https://earth.google.com/)	To study the greater details of the small impact crater under investigation using higher spatial resolution of satellite imagery.
Imagery from CORONA program	Spatial resolution: 1.8 m Mission title: KH-4B Date of acquisition: 01 May 1972 Source: https//earthexplorer.usgs.gov/	To crosscheck the historical existence of the small impact crater under investigation.
Imagery from HiRise camera onboard MRO	Spatial resolution: 0.3 m Source: https://hirise-pds.lpl.arizona.edu	To relate the morphological similarities of impact craters, specifically that were located on the slopes.
Global Digital Elevation Model from ALOS PALSAR	Spatial resolution: 12.5 m Source: https://asf.alaska.edu	To understand the detailed topographic information about the surroundings of the identified small impact crater.
World Hillshade model	World Hillshade layer available from (https://www.arcgis.com)	To perceive the subtle topographic expressions of the identified small impact crater, especially the crater's rim structure and the floor.
Elevations from ICESat-2 photon data	Data product: ATL03 Spatial resolution: 0.7 m Details of acquisitions: $Beam_{ab}$ - 08 Nov. 2021/Track ID: T715 $Beam_{pq}$ - 08 Feb. 2023/Track ID: T768 Downloaded from https://nsidc.org	To generate 2D surface elevation profiles and understand the morphological features of the small impact crater under investigation. ICESat-2 photon-based elevations are available for every 0.7 m distance and should help essay the intricate crater's rim structure and floor morphology variations.

of the structure (like rim-to-rim diameter) from high-resolution satellite imagery. Historical imagery like CORONA, acquired at significant high spatial resolution, can be used to confirm the presence of earth's surface features in the past; thus, in this research, CORONA imagery of ∼1.8 m data acquired during 1972 (nearly 53 years ago) was used to confirm the historical presence of this small impact crater.

The surrounding topography of the identified small-impact crater is mostly sloped. Comparing with a confirmed crater located on a similar topography can help correlate the structural features; for this, imagery from the HiRise camera acquired over a confirmed crater on the Martian surface of sloped terrain was used. During this comparison process, the geomorphological similarities of these two impact craters were interpreted by emphasizing their rim shapes at the uphill and downhill slopes.

ALOS PALSAR GDEM, the best available open-access digital terrain data with a spatial resolution of 12.5 m, was used in this research primarily to understand the surrounding topography of this impact crater. Further, a 3D perspective view was generated from this DEM by overlaying high-resolution satellite imagery. This 3D perspective provided an opportunity to understand the gradient directions of the crater under investigation. Similarly, a hillshade model with a Sun elevation of 45° and a solar azimuth of 315° enabled perceiving the rim and floor of the impact crater with more pronounced.

ICESat-2's Level-2A data product, ATL03, contains height above the WGS84 ellipsoid (ITRF2014 reference frame), latitude, longitude, and time for all photons downlinked by the ATLAS instrument onboard ICESat-

2 observatory[53]. As per the ICESat-2 ATL03's Algorithm Theoretical Basis Document (ATBD), the essential time-variable geophysical parameters will undergo various geophysical and range bias corrections that reduce the errors and identify the signal photons that have accurate elevation information[53]. The ATLAS instrument transmits laser pulses at 10 kHz. At the nominal ICESat-2 orbit altitude of 500 km, approximately one transmitted laser pulse every 0.7 meters along ground tracks is produced, and these pulses are placed into along-track geolocation segments in the data product. From a sequence of elevations retrieved from the along-track geolocated photons, one can generate 2D profiles to understand the earth's surface feature variations. Typically, these 2D profiles have an x-axis as latitude and a y-axis, which contains elevations attributed to the geolocated photons. In this research, two acquisitions of ICESat-2, Beam$_{ab}$ and Beam$_{pq}$, were used to generate 2D profiles over the extent of the small impact crater under investigation. In the context of this research, these profiles can provide a comprehensive assessment of the crater's raised rim and floor's deepest point (that have a lower elevation than the surroundings within the crater's basin).

3. Results

Figure 2 shows a 3D perspective view of the Dhofar impact crater that is being discussed in this research. The 3D perspective was generated using ALOS PALSAR DEM of 12.5 m resolution and is draped with high-resolution satellite imagery. **Figure 3** shows the corresponding slope map (in degrees) that was generated from the same DEM. The placement of the small impact crater lies at the gorge cliff-top – the walls of the gorge are at steep slopes of ∼30°. In turn, the surface over the cliff-top is also a sloped at ∼16°. In a nutshell, approximately 80% of the structure of the impact crater lies on the gentle slopes, and the remaining 20% is on the wall of the gorge - due to this, the final crater shape is neither a circular nor a fully elliptical; however, the structure of this crater has a visually perceivable semi-elliptical rim.

Figure 4 compares the small impact crater on the Dhofar Mountains with an unnamed semi-elliptical crater on the slopes of Tithonium Chasmato, a large Valles Marineris canyon system on Mars. A central inference from this comparison highlights that the craters are semi-elliptical in both cases, with nearly 80% of the raised rim structure perceivable (refer to **Figures 4a,b**). Uphill and downhill landslides were created in both cases due to the ejecta deposition on the inclined slopes. However, in the case of the unnamed crater on Mars, these uphill and downhill landslides are more evident, but in the case of the impact crater of Dhofar Mountains, only traces are visible – possibly due to erosion caused by the weathering and hydrological activity. Importantly, in the case of the impact crater on the Dhofar Mountains, an apparent distortion is observed in the alignment of the fault lines at the area where the downhill landslide is located (refer to **Figures 1c**, **2**, and **4a**).

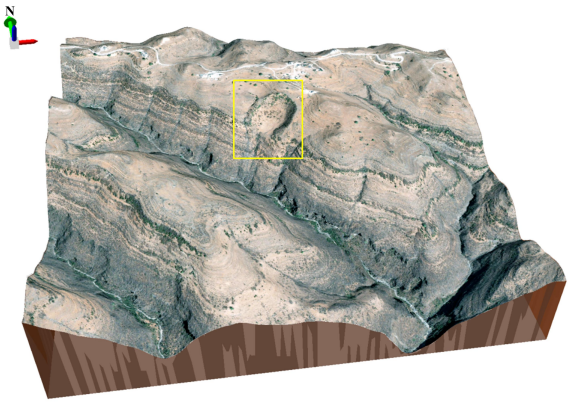


Figure 2. A 3D perspective of the small impact crater on the Dhofar Mountains, above ∼20 km northwest of Salalah, Dhofar Governorate, Sultanate of Oman. The 3D perspective was generated using ALOS PALSAR (12.5 m) DEM and is draped with ESRI satellite imagery base-map.

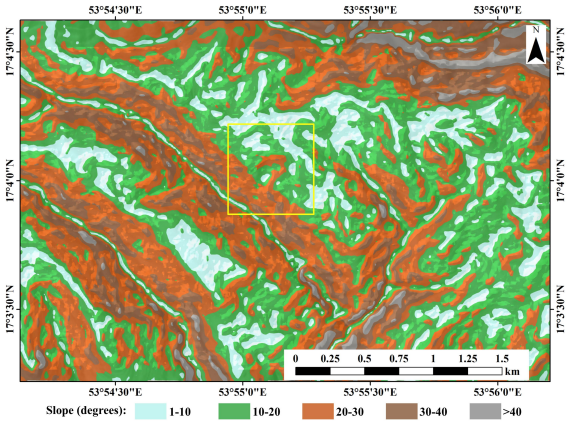


Figure 3. A slope map from the ALOS PALSAR DEM (12.5 m) draped on the corresponding hillshade layer for the extent of the small impact crater on the Dhofar Mountains.

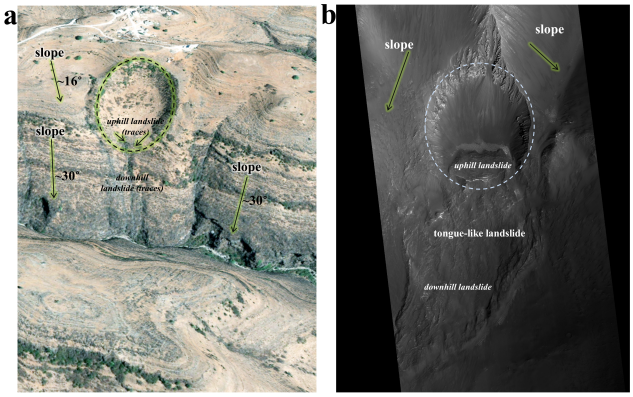


Figure 4. Comparison of the small impact crater on the Dhofar Mountains with that of an unnamed elliptical crater on the slopes of Tithonium Chasmato, a large Valles Marineris canyon system on Mars. (**a**) Small impact crater of Dhofar Mountains as seen in ESRI satellite imagery base-map; (**b**) An unnamed semi-elliptical crater located on the sloped terrain on Mars, as seen in HiRise imagery.

Figure 5a shows the appearance of the small impact crater of Dhofar Mountains in the historical imagery acquired during 1972 (source being CORONA mission, see **Table 1**) – the shape of the crater under investigation is highly evident in this historical imagery. **Figure 5b** shows the hillshade map of the study area where the crater's physical features, like the rim, basin floor, and tongue-like landslide at the downhill, are highly perceived.

As discussed in the datasets and methods sections, in this research, two beams (Beam$_{ab}$ and Beam$_{pq}$) of ICESat-2 photon data were used to generate along-track elevation profiles over the Dhofar impact crater under investigation. These profiles are shown in **Figure 6**. **Figure 6a** shows the satellite imagery for the extent of the study area overlaid with two-photon beams acquired by ICESat-2. **Figures 6b,c** show the 2D elevation profiles generated for the Beam$_{ab}$ and Beam$_{pq}$, respectively. The primary observation from these profiles is that the rim-to-rim distance (D) is not constant; as obtained from Beam$_{ab}$, D is 255 m, whereas it is 260 m from Beam$_{pq}$. In the scenario of the crater being circular, then in general, D, the rim-to-rim distance or the diameter of the crater will usually be uniform. In the case of this crater on the Dhofar Mountains, the rim is not circular but near-elliptical; thus, variation exists in the D. Also. Generally, the maximum depth point in a circular impact crater lies at its center, whereas, for this crater, it is observed that the deepest point with a depth of 35 m (refer to **Figures 6a,b**) is shifted downhill.

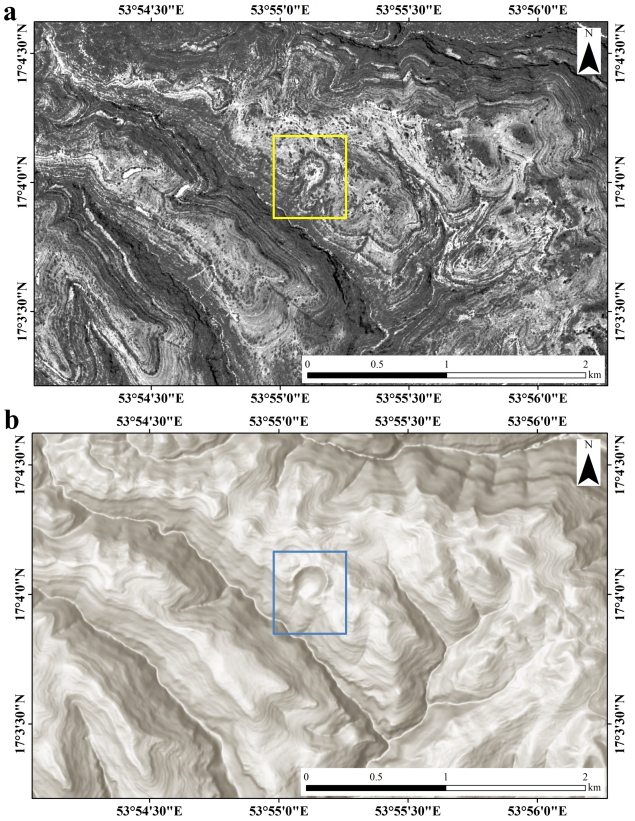


Figure 5. An impact crater on the Dhofar Mountains as seen in the historical imagery, and its corresponding topographic hillshade map highlights the crater's rim structure and the basin floor. (**a**) Imagery from the CORONA mission acquired in 1972; (**b**) Hillshade map for the extent of the Dhofar Mountains crater (Source: ESRI World Hillshade layer).

The crater rim, which is the crater's edge, is typically an elevated surface from the basin, and within the rim structure, the line of maximum elevation is termed crest. For the Dhofar impact crater, the rim crest is elevated ∼7 m on the uphill side but is sharp (abrupt), whereas the rim crest's elevation is ∼20 m on the downhill side but is smooth. From the high-resolution satellite imagery, it is observed that vegetation exists on the internal slopes towards the upper side of the cavity from the rim crest.

The experimental setup (in a sandbox - granular target surface), which consists of the simulated landscape environment of the crater on the Dhofar Mountains, is shown in **Figure 7**.

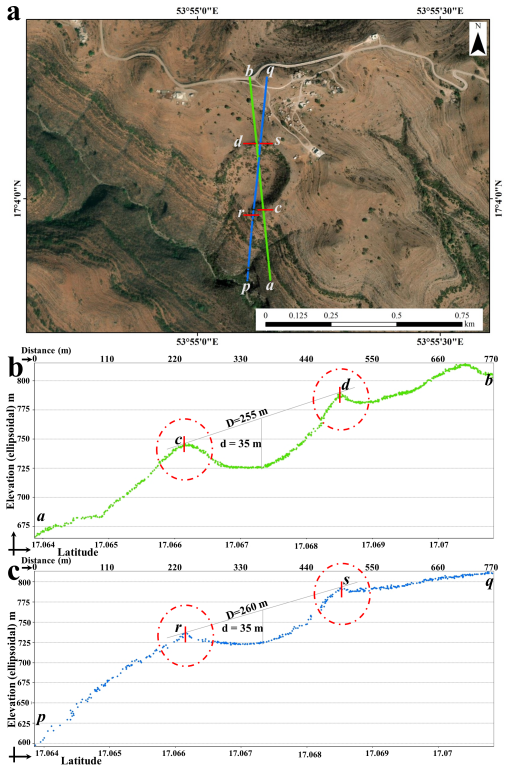


Figure 6. 2D cross-sectional elevation profiles generated using along-track ICESat-2 photon beams for the impact crater at Dhofar Mountains. (**a**) High-resolution satellite image overlaid with two ICESat-2 photon beams; (**b**) 2D elevation profile for Beam$_{ab}$; (**c**) 2D elevation profile for the Beam$_{pq}$. Dashed circles in the profile diagrams highlight the raised rims of the impact crater.

Figure 7a shows the landscape before the impact, and **Figure 7b** shows a frame captured during the post-contact and ejection stages. **Figure 7c** is the final form of the landscape after the impact; an elliptical impact crater with a crescent-shaped rim, the occurrence of the deepest point towards the downhill, and tongue-like landslide are evident in the post-impact landscape. Notably, a distortion of the simulated folds, especially at the tongue-like landslide, is observed in the post-impact landscape (refer to **Figure 7c**).

4. Discussion

Most impact craters on planetary surfaces are circular, as most projectile strikes at an oblique angle following the laws of celestial mechanics. Only 5% of the crater-records data (especially on Mars, Moon, and Venus) show an elliptical morphology [50, 54–56]. Numerical simulations proved that the elliptical craters result from impacts that occur at a very shallow angle of incidence (say 12°) as the resulting crater shape deviates from a circular symmetry and becomes elongated in the direction of impact [8, 13, 17, 18, 50, 54]. The ellipticity of the crater increases with decreasing impact angle [50, 56, 57]. Importantly, even if the impact strike is from an oblique angle on a target surface with rugged terrain or sloped topography, at a local scale, the impact of the extraterrestrial objects will be apparently a shallower one with respect to the sloped target surface. The peculiarity of the impact crater discussed in this research is that it lies on a sloped terrain and the edge of a cliff-top, with ∼80% of the crater floor on a ∼16° slope; thus, it is a near-elliptical crater which is evident in the high-resolution satellite imagery (refer to **Figures 1c** and **2**). The remaining ∼20% of the crater floor formation failed due to the gorge's steep slope.

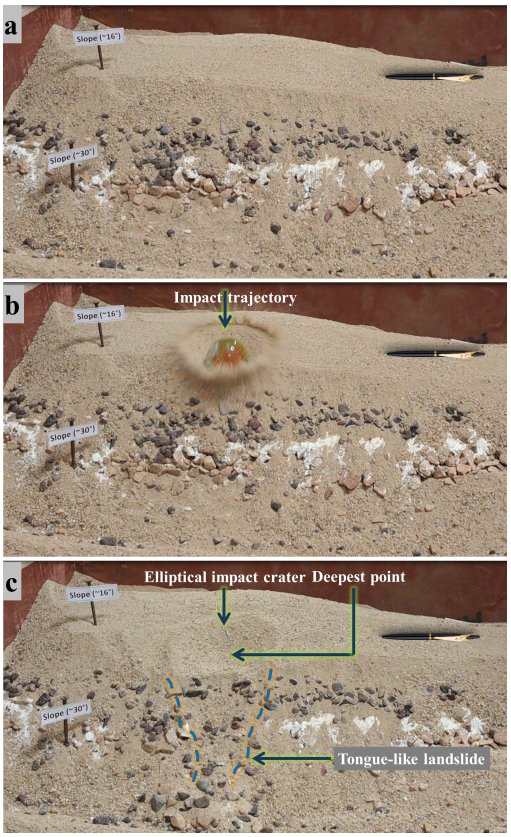


Figure 7. A sandbox (granular target surface) experiment to simulate impact cratering on slopes. (**a**) Pre-impact landscape; (**b**) Frame showing contact and ejection stage. (**c**) Post-impact landscape showing crescent shaped rim, deepest point, and tongue-like landslide distorting the folds in the subsurface.

Aschauer and Kenkmann investigated the effect of surface topography on crater formation and systematically studied impact cratering processes on inclined hill-

sides up to 25° slopes utilizing analogue experiments [18]. Their experiments concluded that the transient crater develops roughly symmetrically perpendicular to the sloping plane, resulting in higher ejection angles uphill than downhill when measured with respect to a horizontal plane. At slope angles close to the angle of repose of the respective bulk solids, the aspect ratios of the craters can reach ~1.7. Uphill-downhill cross sections become increasingly asymmetric, the depth-diameter ratio of the crater decreases, and the deepest point shifts downhill with increasing slope angle. Mass wasting is initiated both in the uphill and downhill sectors of the crater rim. The landslides emanating from the uphill rim for steep slopes can overshoot the crater cavity and superpose the downhill crater rim in a narrow tongue. Mass wasting initiated at the downhill sector forms a broader and shallower tongue and is triggered by ejecta deposition on the inclined slope [18].

Figure 8 is a map showing the dimensions of the impact crater under investigation. Due to the crater's position on the cliff-top edge, the elliptical rim is incomplete due to the formation of a narrow tongue at steep slopes of the gorge wall. The distance from the perceivable rim structure to the start of the narrow tongue (assuming it is the major axis of the crater) is ~259 m, and the rim-to-rim distance, i.e., the minor axis, is ~212 m; thus, the ellipticity (ε) of this crater is nearly 1:1.22. Bottke et al. suggested that a crater can be termed as an elliptical if the major axis is at least 120 % of the minor axis [56]. The deepest point (d = 35 m) of this small impact crater is seen to be shifted downhill (refer to **Figures 6** and **8**), which is a characteristic feature that is in line with the observations made by Aschauer and Kenkmann in their experiment for simulating impact craters on slopes [18]. The Dhofar impact crater's depth-diameter (d/D) ratio is 1:7.4 if D is the apparent major axis and 1:6 for the minor axis; these values agree with the mechanics of small impact craters [8].

The rim crest, the crater's edge typically elevated above the original surface, is one of the primary morphological features that acts as a key interpreter while detecting impact craters in the imageries through remote sensing methods. Impact cratering experiments over sloped surfaces conducted by Aschauer & Kenkmann and Hayashi & Sumita have proved that the crater floor steepens on the upslope side and a thick rim forms on the downslope side, thus forming an asymmetric profile [18, 51]. 2D elevation profiles obtained from the ICESat-2 photons over the extent of the Dhofar impact crater in this research exhibit a steeper floor on the upslope side and the rim getting thicker on the downslope side (refer to **Figure 6b**). Thus, the observation retrieved in this research is well in tune with the numerical simulations done on the sloped surface. Moreover, the rim of the small impact crater in this research is thicker on the downslope side and thinner on the upslope side such that it forms a crescent shape (refer to **Figures 6b,c**); this observation was also noted by Aschauer & Kenkmann and Hayashi & Sumita in their experiments [18, 51]. Krohn et al., while analyzing 2892 asymmetric craters on asteroid Vesta, observed that they are mainly characterized by a sharp crater rim on the uphill side and a smooth one on the downhill side [58]. The details given by Krohn et al., results from the experiments of Aschauer & Kenkmann and Hayashi & Sumita, and the morphological features of the impact crater described in this research are all in sync [18, 51, 58]. However, because the impact crater described in this research is on the edge of the cliff-top, the completeness of the elliptical crater rim is lacking, but the phenomenon of tongue-like landslide at the downslope side as described by the Aschauer & Kenkmann is well observed (refer to **Figure 4**) [18].

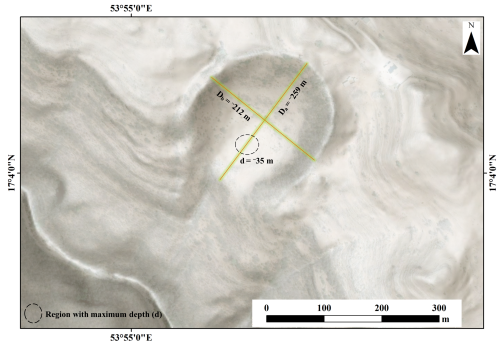


Figure 8. A sketch map showing the dimensions of the impact crater located on the sloped terrain and the edge of a cliff-top. (Dhofar Mountains, Dhofar Governorate, Sultanate of Oman).

One noteworthy observation from this research is the distortion in the subsurface folds (supposed to be monoclines) that is majorly evident in the tongue-like

landslide section (refer to **Figures 2** and **4a**). As done in this research, results from the experimental setup with a simulated landscape environment with that of the Dhofar impact crater underpins the consequences of the impact on slopes (refer to **Figure 7**). **Figure 7c**, which shows the final form of the landscape after the impact (in experimental setup), highlights the evidence of a crescent-shaped rim, the shifting of the deepest point towards the downhill, and a tongue-like landslide. Notably, the distortion of the simulated folds, especially at the tongue-like landslide, is observed in the post-impact landscape. Studies related to the impact craters and their consequences on the subsurface folds are rare; thus, the Dhofar impact crater, because of its location on a gorge's cliff-top edge, offers an intriguing window (cross-sectional view) to study the distortions of sub-surface folds associated with the impact craters - but for this extensive fieldwork is a need. Ignoring the sizes of the impact craters on the Dhofar Mountains and that of the unnamed Martian impact crater (confirmed by Aschauer and Kenkmann), which is also in a similar sloped terrain, the morphological features are similar to each other [18].

Research by Zerboni et al. has proven that the rugged terrains of Dhofar Mountain have been almost uninhabited since the Paleolithic and Neolithic periods [30]. Also, in this research, the verification of the small impact crater's structure during 1972 through the historical imagery confirms that the structure is not altered, which affirms it is not a man-made one.

High-resolution satellite imagery of the Dhofar impact crater shows a series of features oriented radially and concentrically toward the rim (outwards) – these features are, in general, the result of ballistics radial flow during the excavation stage of the crater formation. Also, vegetation is seen near the rim of this small impact crater, and most of the region outside the crater is almost free of trees (refer to **Figures 4a** and **6a**). Cockell and Lee, in their research, observed that the raised rim of a crater system can be the first to be influenced by the aeolian activity that will aid in trapping the soils in the gaps of bedrock – this, in turn, will provide an ecosystem that can support vegetation [23]; this is the reason vegetation is seen near the rim of the Dhofar impact crater.

In this research, the optical high-resolution satellite imagery like IRS Resroucesat-2A LISS-IV, online satellite imagery base-maps, and archival imagery from the CORONA program confirms the structure of the Dhofar impact crater due to its surface expression acting as an interpretation key. Imagery from the HiRise camera showing a confirmed impact crater on Mars located on similar geological settings like that of the impact crater under investigation helped to deduce the similarities between them. Global DEM of 12.5 m from ALOS PALASR and the World Hillshade model has aided in envisaging the study area in a 3D perspective and in perceiving the topographic expression of the small impact crater. Notably, the 0.7 m spaced elevation profiles from ICESat-2 photon data have enabled us to understand the along-track morphological features of this unique small-impact crater. Together with the results and observations from the experiments done by earlier researchers and the impact simulation in a sandbox experiment as done in this research, confirms the final formation of a near-elliptical and crescent-shaped simple (non-complex) crater system on the target surface if the impact collision happens on slopes and edge of the gorge's cliff-top.

5. Conclusions

Research on extraterrestrial impacts enhances our understanding of the Solar System's history, planets' thermodynamic processes, and life's evolution.

A surface expression representing a small impact crater is discovered on the slopes of the Dhofar Mountains, located in the Dhofar Governorate of Sultanate of Oman. The location of the identified small impact crater is $\sim$20 km to the northwest of Salalah city. In this article, we described the interpreted morphological features of this small-impact crater using remote sensing-based methods, archived imagery originally acquired for reconnaissance survey, open access GDEM, World hillshade dataset, and high-resolution ICESat-2 photons-based along-track elevations. Notably, the high-resolution 2D profiles from ICESat-2 photon data helped essay the along-track elevation profile of the crater's structure from rim-to-rim along with the deepest point.

Besides the difference in size, this impact crater mostly resembles an unnamed impact crater located on the slopes of Tithonium Chasmato on Mars, which is confirmed through the HiRise imagery.

The morphological features of this impact crater, especially the rim structure, occurrence of the deepest point, and the tongue-like landslide at the downhill, are well in sync with the results and observations done earlier by the researchers through numerical simulations and also proven to be in line with the impact simulation done in a sandbox experiment as performed in this study.

Although the crater described in this research is near-elliptical and crescent, it is one of the rarest on Earth, and its peculiarity is that it is also lying on sloped terrain and the edge of a cliff-top. Interestingly, the steeped slope of this gorge wall exposes the folds; this feature enables one to study the bearing of extraterrestrial impact on the subsurface features – this can be a future scope of this study.

Our study reviewed the morphological features of the Dhofar impact crater through a remote sensing perspective. The details regarding the angle of the impactor, its dimensions, and the crater's age are not studied in this research – this is a limitation of this study, and further scientific investigations are called upon with extensive fieldwork and material analysis.

Author Contributions

Conceptualization, G.D. and S.K.S.; methodology, G.D., A.K.B., and S.K.S.; software, G.D., O.S.G., and S.R.; validation, G.D., A.K.B., and S.K.S.; formal analysis, G.D., O.S.G., S.R., and A.K.B.; investigation, G.D., O.S.G., and S.R.; resources, A.K.B.; data curation, O.S.G. and S.R.; writing—original draft preparation, G.D.; writing—review and editing, G.D., S.R. and S.K.S.; visualization, G.D., O.S.G., and S.R.; supervision, S.K.S.; project administration, A.K.B. All authors have read and agreed to the published version of the manuscript.

Funding

This research received no external funding.

Institutional Review Board Statement

Not applicable.

Informed Consent Statement

Not applicable.

Data Availability Statement

Indian Remote Sensing (IRS) Resourcesat-2A Linear Imaging Self Scanner-4 (LISS-4) products can be found in the web portal at https://bhoonidhi.nrsc.gov.in maintained by National Remote Sensing Centre (NRSC). Base-maps comprising high-resolution satellite imagery were accessible from OpenGIS Web Map Service Interface Standard (WMS) supported by ArcGIS Online Base-maps (https://www.arcgis.com) and Google Earth (https://www.opengee.org). These base-map layers were accessed in ESRI's ArcGIS Pro 10.3 version. Additionally, the World Hillshade layer was considered from the ArcGIS Online base-maps. Historical imagery from the CORONA mission was accessible from https://earthexplorer.usgs.gov/. HiRise imagery specified in this research can be accessed from https://www.uahirise.org, maintained by the University of Arizona. The open-accessible global digital elevation model used in this research is ALSO PALSAR GDEM of 12.5 m and can be accessed from https://asf.alaska.edu, maintained by Alaska Satellite Facility. Level-2A ATL03 data product of ICESat-2 can be found in the NASA National Snow and Ice Data Center Distributed Active Archive Centre (NSIDC DAAC) available at https://nsidc.org/data/icesat-2.

Acknowledgments

The authors gratefully acknowledge Dr. Prakash Chauhan, Director, National Remote Sensing Centre, ISRO, Hyderabad, for providing the infrastructure for this research. Similarly, the authors sincerely thank the HiRise and Bhoonidhi science teams for providing access to their original data sources. We acknowledge the continued support and scientific insights from Mr. Sagar

S Salunkhe, Mr. Rakesh Fararoda, Mr. Hansraj Meena, and other staff members of Regional Remote Sensing Centre—West, NRSC/ISRO, Jodhpur. The authors would like to mention a special thanks to Mr. Gaurav Kumar, Scientist, IN-SPACe, India, for providing design and setting up the infrastructure for the sandbox experiment described in this research.

Conflicts of Interest

The authors declare no conflict of interest.

References

[1] Erickson, J., 2001. Quakes, eruptions, and other geologic cataclysms: revealing the earth's hazards. Facts on File: New York, USA. pp. 1–309.

[2] Brunsden, D., 2001. A critical assessment of the sensitivity concept in geomorphology. Catena. 42(2–4), 99–123. DOI: https://doi.org/10.1016/S0341-8162(00)00134-X

[3] Pike, R.J., 1980. Formation of complex impact craters: Evidence from Mars and other planets. Icarus, 43(1), 1–19. DOI: https://doi.org/10.1016/0019-1035(80)90083-4

[4] Graham, G.A., Kearsley, A.T., Grady, M.M., Wright, I.P., Griffiths, A.D., McDonnell, J.A.M., 1999. Hypervelocity impacts in low Earth orbit: Cosmic dust versus space debris. Advances in Space Research. 23(1), 95–100. DOI: https://doi.org/10.1016/S0273-1177(98)00235-X

[5] Humes, D.H., 1992. Large craters on the meteoroid and space debris impact experiment. In: Levine, A.S. (ed.). LDEF: 69 Months in Space. First Post-Retrieval Symposium, part 1. National Aeronautics and Space Administration: Washington, DC, USA. pp. 399–418.

[6] Campbell, J.W., Phipps, C., Smalley, L., Reilly, J., Boccio, D., 2003. The impact imperative: laser ablation for deflecting asteroids, meteoroids, and comets from impacting the earth. AIP conference proceedings. 664(1), 509–522.

[7] Boyce, J.M., Wilson, L., Mouginis-Mark, P.J., Hamilton, C.W., Tornabene, L.L., 2012. Origin of small pits in Martian impact craters. Icarus. 221(1), 262–275. DOI: https://doi.org/10.1016/j.icarus.2012.07.027

[8] Osinski, G.R., Grieve, R.A.F., Ferrière, L., et al., 2022. Impact Earth: A review of the terrestrial impact record. Earth-Science Reviews. 232, 104112. DOI: https://doi.org/10.1016/j.earscirev.2022.104112

[9] Tancredi G., Ishitsuka, J., Schultz, P.H., et al., 2009. A meteorite crater on Earth formed on September 15, 2007: The Carancas hypervelocity impact. Meteoritics & Planetary Science. 44(12), 1967–1984. DOI: https://doi.org/10.1111/j.1945-5100.2009.tb02006.x

[10] Bartoschewitz, R., Appel, P., Barrat, J.A., et al., 2017. The Braunschweig meteorite– a recent L6 chondrite fall in Germany. Geochemistry. 77(1), 207–224. DOI: http://dx.doi.org/10.1016/j.chemer.2016.10.004

[11] Suzuki, A.I., Fujita, Y., Harada, S., et al., 2021. Experimental study concerning the oblique impact of low-and high-density projectiles on sedimentary rocks. Planetary and Space Science. 195, 105141. DOI: https://doi.org/10.1016/j.pss.2020.105141

[12] Pilkington, M., Grieve, R.A.F., 1992. The geophysical signature of terrestrial impact craters. Reviews of Geophysics. 30(2), 161–181. DOI: https://doi.org/10.1029/92RG00192

[13] Kenkmann, T., Poelchau, M.H., Wulf, G., 2014. Structural geology of impact craters. Journal of Structural Geology. 62, 156–182. DOI: https://doi.org/10.1016/j.jsg.2014.01.015

[14] Melosh, H.J., Ivanov, B.A., 1999. Impact crater collapse. Annual Review of Earth and Planetary Sciences. 27(1), 385–415. DOI: https://doi.org/10.1146/annurev.earth.27.1.385

[15] Collins, G.S., Melosh, H.J., Osinski, G.R., 2012. The impact-cratering process. Elements. 8(1), 25–30. DOI: https://doi.org/10.2113/gselements.8.1.25

[16] Holsapple, K.A., Housen, K.R., 2007. A crater and its ejecta: An interpretation of Deep Impact. Icarus. 191(2), 586–597. DOI: https://doi.org/10.1016/j.icarus.2006.08.035

[17] Herrick, R. R., Forsberg-Taylor, N. K. 2003. The shape and appearance of craters formed by oblique impact on the Moon and Venus. Meteoritics & Planetary Science. 38(11), 1551–1578. DOI: https://doi.org/10.1111/j.1945-5100.2003.tb00001.x

[18] Aschauer, J., Kenkmann, T., 2017. Impact cratering on slopes. Icarus. 290, 89–95. DOI: http://dx.doi.org/10.1016/j.icarus.2017.02.021

[19] Al Shehri, A. A., 2024. Mapping moon craters: Scientific knowledge from 1965 to 2022: Systematic review. The Egyptian Journal of Remote Sensing and Space Sciences. 27(2), 456–465. DOI: https://doi.org/10.1016/j.ejrs.2024.04.001

[20] Salamunićcar, G., Lončarić, S., Pina, P., Bandeira, L., Saraiva, J., 2011. MA130301GT catalogue of Martian impact craters and advanced evaluation of crater detection algorithms using diverse topography and image datasets. Plane-

tary and Space Science. 59(1), 111–131. DOI: https://doi.org/10.1016/j.pss.2010.11.003

[21] Wright, S.P., Tornabene, L.L., Ramsey, M.S., 2013. Remote sensing of impact craters. In: Osinski, G.R., Pierazzo, E. (eds.). Impact cratering: Processes and products. Wiley-Blackwell Publishing Ltd: NJ, USA. pp. 194–214.

[22] Yue, Z., Shi, K., Di, K., Lin, Y., Gou, S., 2023. Progresses and prospects of impact crater studies. Science China Earth Sciences. 66(11), 2441–2451. DOI: https://doi.org/10.1007/s11430-022-1009-0

[23] Cockell, C.S., Lee, P., 2002. The biology of impact craters–a review. Biological Reviews. 77(3), 279–310. DOI: https://doi.org/10.1017/S146479310100584X

[24] Reimold, W.U., 1995. Impact cratering-a review, with special reference to the economic importance of impact structures and the Southern African impact crater record. Earth, Moon, and Planets. 70(1), 21–45. DOI: https://doi.org/10.1007/BF00619449

[25] Velázquez, V. F., Colonna, J., Sallun, A. E. M., et al., 2014. The Colônia impact crater: geological heritage and natural patrimony in the southern metropolitan region of São Paulo, Brazil. Geoheritage. 6(4), 283–290. DOI: https://doi.org/10.1007/s12371-014-0121-0

[26] Searle, M., 2019. Geology of the Oman mountains, eastern Arabia. Springer: New York, USA. pp. 478.

[27] Rose, J.I., Usik, V.I., Hilbert, Y., et al., 2023. Prehistoric settlement patterns in southern Oman from the Lower Palaeolithic to the Neolithic. Paléorient. 49(1), 9–34. DOI: https://doi.org/10.4000/paleorient.2774

[28] Charpentier, V., Maiorano, M. P., Marchand, G., Vosges, J., Borgi, F., 2023. Twelve years of the 'Arabian Seashores' project: How the extensive investigation of coastal Oman changed the paradigm of the Arabian Neolithic. Arabian Archaeology and Epigraphy. 34(S1), S1–S21. DOI: https://doi.org/10.1111/aae.12236

[29] Cremaschi, M., Zerboni, A., Charpentier, V., et al., 2015. Early–Middle Holocene environmental changes and pre-Neolithic human occupations as recorded in the cavities of Jebel Qara (Dhofar, southern Sultanate of Oman). Quaternary International. 382, 264–276. DOI: http://dx.doi.org/10.1016/j.quaint.2014.12.058

[30] Zerboni, A., Perego, A., Mariani, G. S., et al., 2020. Geomorphology of the Jebel Qara and coastal plain of Salalah (Dhofar, southern Sultanate of Oman). Journal of Maps. 16(2), 187–198. DOI: https://doi.org/10.1080/17445647.2019.1708488

[31] Yue, S., He, L., Wen, Y., Lu, G., Lin, H., 2013. Shape characteristics-based extraction of lunar impact craters: using DEM from the Chang'E-1 satellite as a data source. Annals of GIS. 19(1), 53–62. DOI: https://doi.org/10.1080/19475683.2012.758656

[32] Christian, J. A., Derksen, H., Watkins, R. 2021. Lunar crater identification in digital images. The Journal of the Astronautical Sciences. 68(4), 1056–1144. DOI: https://doi.org/10.1007/s40295-021-00287-8

[33] Pedrosa, M.M., de Azevedo, S.C., da Silva, E.A., Dias, M.A., 2017. Improved automatic impact crater detection on Mars based on morphological image processing and template matching. Geomatics, Natural Hazards and Risk. 8(2), 1306–1319. DOI: https://doi.org/10.1080/19475705.2017.1327463

[34] Urbach, E.R., Stepinski, T.F. 2009. Automatic detection of sub-km craters in high resolution planetary images. Planetary and Space Science. 57(7), 880–887. DOI: https://doi.org/doi:10.1016/j.pss.2009.03.009

[35] Zhou, Y., Zhao, H., Chen, M., Tu, J., Yan, L., 2018. Automatic detection of lunar craters based on DEM data with the terrain analysis method. Planetary and Space Science. 160, 1–11. DOI: https://doi.org/10.1016/j.pss.2018.03.003

[36] Zhang, S., Zhang, P., Yang, J., et al., 2024. Automatic detection for small-scale lunar impact crater using deep learning. Advances in Space Research. 73(4), 2175–2187. DOI: https://doi.org/10.1016/j.asr.2023.05.041

[37] Comer, D.C., Harrower, M.J. 2013. Mapping archaeological landscapes from space. Springer: New York, USA. pp. 276.

[38] Delamere, W.A., Tornabene, L.L., McEwen, A.S., et al., 2010. Color imaging of Mars by the high resolution imaging science experiment (HiRISE). Icarus. 205(1), 38–52. DOI: https://doi.org/10.1016/j.icarus.2009.03.012

[39] Dundas, C.M., Byrne, S., McEwen, A.S., et al., 2014. HiRISE observations of new impact craters exposing Martian ground ice. Journal of Geophysical Research: Planets. 119(1), 109–127. DOI: https://doi.org/10.1002/2013JE004482

[40] Xin, X., Di, K., Wang, Y., et al., 2017. Automated detection of new impact sites on Martian surface from HiRISE images. Advances in Space Research. 60(7), 1557–1569. DOI: https://doi.org/10.1016/j.asr.2017.06.044

[41] Watters, W.A., Geiger, L.M., Fendrock, M., Gibson, R., 2015. Morphometry of small recent impact craters on Mars: Size and terrain dependence, short-term modification. Journal of Geophysical Research: Planets. 120(2), 226–254. DOI: https://doi.org/10.1002/2014JE004630

[42] Gottwald, M., Fritz, T., Breit, H., et al., 2017. Re-

mote sensing of terrestrial impact craters: The TanDEM-X digital elevation model. Meteoritics & Planetary Science. 52(7), 1412–1427. DOI: https://doi.org/10.1111/maps.12794

[43] Liu, D., Chen, M., Qian, K., et al., 2017. Boundary detection of dispersal impact craters based on morphological characteristics using lunar digital elevation model. IEEE Journal of Selected Topics in Applied Earth Observations and Remote Sensing. 10(12), 5632–5646. DOI: https://doi.org/10.1109/JSTARS.2017.2749403

[44] Indu, G.K., James, S., Chandran, S.R., et al., 2022. Deriving a denudation index for terrestrial meteorite impact craters using drainages as proxies. Geomorphology. 397, 108007. DOI: https://doi.org/10.1016/j.geomorph.2021.108007

[45] Markus, T., Neumann, T., Martino, A., et al., 2017. The Ice, Cloud, and land Elevation Satellite-2 (ICESat-2): science requirements, concept, and implementation. Remote sensing of environment. 190, 260–273. DOI: https://doi.org/10.1016/j.rse.2016.12.029

[46] Magruder, L., Neumann, T., Kurtz, N., 2021. ICESat-2 Early Mission Synopsis and Observatory Performance. Earth and Space Science. 8(5), e2020EA001555. DOI: https://doi.org/10.1029/2020EA001555

[47] Dandabathula, G. 2022. Applications of ICES at-2 Photon Data in the Third Pole Environment. In Pandey, M., Pandey, P.C., Ray, Y., et al. (eds.). Advances in remote sensing technology and the three poles. Wiley. pp. 213–229. DOI: https://doi.org/10.1002/9781119787754.ch14

[48] Brown, M.E., Arias, S.D., Chesnes, M., 2023. Review of ICESat and ICESat-2 literature to enhance applications discovery. Remote Sensing Applications: Society and Environment. 29, 100874. DOI: https://doi.org/10.1016/j.rsase.2022.100874

[49] Schultz, P.H., Eberhardy, C.A., Ernst, C.M., et al., 2007. The Deep Impact oblique impact cratering experiment. Icarus. 191(2), 84–122. DOI: http://dx.doi.org/10.1016/j.icarus.2007.06.031

[50] Michikami, T., Hagermann, A., Morota, T., et al., 2017. Oblique impact cratering experiments in brittle targets: Implications for elliptical craters on the Moon. Planetary and Space Science. 135, 27–36. DOI: http://dx.doi.org/10.1016/j.pss.2016.11.004

[51] Hayashi, K., Sumita, I., 2017. Low-velocity impact cratering experiments in granular slopes. Icarus. 291, 160–175. DOI: http://dx.doi.org/10.1016/j.icarus.2017.03.027

[52] Herrick, R.R., Forsberg-Taylor, N.K., 2003. The shape and appearance of craters formed by oblique impact on the Moon and Venus. Meteoritics & Planetary Science. 38(11), 1551–1578. DOI: https://doi.org/10.1111/j.1945-5100.2003.tb00001.x

[53] Neumann, T.A., Brenner, A., Hancock, D., Robbins, J., Gibbons, A., Lee, J., Harbeck, K., Saba, J., Luthcke, S.B. Rebold, T., 2023. ATLAS/ICESat-2 L2A Global Geolocated Photon Data. (ATL03, Version 6). NASA National Snow and Ice Data Center Distributed Active Archive Center: Boulder, Colorado USA. DOI: https://doi.org/10.5067/ATLAS/ATL03.006

[54] Elbeshausen, D., Wünnemann, K., Collins, G.S., 2013. The transition from circular to elliptical impact craters. Journal of Geophysical Research: Planets. 118(11), 2295–2309. DOI: https://doi.org/10.1002/2013JE004477

[55] Collins, G.S., Elbeshausen, D., Davison, T.M., et al., 2011. The size-frequency distribution of elliptical impact craters. Earth and Planetary Science Letters. 310(1–2), 1–8. DOI: https://doi.org/10.1016/j.epsl.2011.07.023

[56] Bottke Jr, W.F., Love, S.G., Tytell, D., Glotch, T., 2000. Interpreting the elliptical crater populations on Mars, Venus, and the Moon. Icarus. 145(1), 108–121. DOI: https://doi.org/10.1006/icar.1999.6323

[57] Gault, D.E., Sonett, C.P. 1982. Laboratory simulation of pelagic asteroidal impact: Atmospheric injection, benthic topography, and the surface wave radiation field. In: Silver, L.T., Schultz, P.H. (eds.). Geological implications of impacts of large asteroids and comets on the Earth. Geological Society of America: Bolder, CO, USA. pp. 69–92

[58] Krohn, K., Jaumann, R., Elbeshausen, D., et al., 2014. Asymmetric craters on Vesta: Impact on sloping surfaces. Planetary and Space Science. 103, 36–56. DOI: https://doi.org/10.1016/j.pss.2014.04.011